mRNA and drug delivery with lipid-based nanoparticles

Zeng, Y.

Chapter 4

Efficient mRNA Delivery to Cardiomyocytes *in vitro* Using Fusogenic LNPs

Abstract

Heart failure usually results from the loss of billions of specialized cardiac muscle cells known as cardiomyocytes (CMs), in a process induced by myocardial infarction (MI). To minimize health issues relating to the loss of cardiomyocytes, cardiac tissue repair is essential. However, optimizing cardiac tissue repair is difficult. This process could be improved by transient mRNA expression that regulates the behavior and fate of progenitor cells, thus a robust mRNA therapy could result in the regeneration of lost myocardium. Cardiomyocytes derived from induced pluripotent stem cells (iPSC-CMs) represent the best cell source for cardiac regeneration but require efficient mRNA delivery. To date, lipid nanoparticles (LNPs) represent the most efficient mRNA delivery platform. However, the transfection efficiency of LNPs is still hampered by endosomal entrapment after endocytosis by the cells. Enhanced mRNA transfection efficiency has been achieved by the introduction of fusogenic coiled-coil peptides into LNPs. Here, we modified LNPs with the coiled-coil peptide CPE4, while iPSC-CMs were pretreated with the complementary coiled-coil peptide CPK4, and we achieved improved mRNA transfection efficiency. Different incubation methods of coiled-coil peptide-modified LNPs were compared, and it was shown that the 1-step incubation protocol achieved a higher mRNA transfection efficiency. mRNA transfection enhancement of iPSC-CMs using this 1-step incubation protocol was independent of the LNP lipid composition. This study shows that the modification of LNPs with fusogenic coiled-coil peptides significantly improved mRNA expression in iPSC-CMs and holds great promise for future heart regenerative therapies.

Introduction

Heart failure is a leading cause of morbidity and mortality worldwide.[1] In Europe alone, more than 3.5 million people are diagnosed with heart failure every year; 50% of these will die within 4 years.[2,3] Moreover, due to aging and improved survival after myocardial infarction (MI), the incidence and prevalence of heart failure is increasing. To date, there is no cure, and treatment options are limited to drug therapies and a limited number of heart transplantations. One of the main causes leading to heart failure is the massive loss of cardiomyocytes (*i.e.* heart muscle cells) as a result of acute or chronic ischemia. Because the adult mammalian heart has limited capacity for regeneration after MI,[4] this loss of cardiomyocytes is considered to be irreversible, eventually leading to a loss of pump function and heart failure. Existing medical and device-based therapies can ameliorate the effects of heart failure but cannot regenerate the loss of functional myocardium.[5] Endogenous replenishment of cardiomyocytes is insufficient to repair the myocardial injury after MI, thus efficient delivery systems can deliver DNA, RNA, or proteins with specific functions to induce cardiac repair and ultimately facilitate regeneration of cardiomyocytes to rescue the ischemic myocardium are needed.[6]

Primary cardiomyocytes are difficult to isolate and have a short lifespan, thus many techniques have been adopted to obtain reliable sources of human cardiomyocytes, including bone marrow-derived, embryonic stem cells (ESCs), and induced pluripotent stem cells (iPSCs).[7,8] iPSC-derived cardiomyocytes (iPSC-CMs) are the most promising cell source for cardiac repair research, as they can proliferate indefinitely and differentiate into cardiac lineages, including cardiomyocytes, smooth muscle cells, endothelial cells, and cardiac progenitors.[9-11] iPSC-CMs mimic primary cardiac cell functional performance by expressing the correct electrical and physiological properties of the developing heart, which makes iPSCs an advantageous candidate for preclinical drug screening and cardiac research about signaling pathways that underpin myocardial development.[8,12,13]

Cardiac-specific protein expression, such as Yes-associated protein (YAP), VEGF, and angiopoietin-1 (Ang1), in adult mice could drive cardiomyocyte proliferation and improve cardiac function after MI.[14-19] The cardiac-specific protein expression needs to be tightly controlled, since continuous expression may lead to uncontrolled cardiac repair.[17] Fortunately, messenger RNA (mRNA) activity is temporary as a result of its natural degradation, allowing temporal control over protein expression to stimulate regeneration while avoiding uncontrolled long-term growth. mRNA therapeutics have shown the ability to induce vascular regeneration after myocardial infarction *in vitro* and *in vivo*.[16,20-22] However, the major challenge remaining is the delivery of relevant therapeutic doses of mRNA to cardiomyocytes *in vivo*. For efficient functional cytosolic delivery to, and release within, target cells these highly charged, immunogenic, and membrane-impermeable mRNA molecules require the use of delivery systems.[23,24] To this end, lipid nanoparticles (LNPs) serve as the state-of-the-art vector that can package, protect and release RNA molecules inside cells.[25] LNPs have realized the translation of RNA therapeutics to the clinic, highlighted by the successful use of the LNP-siRNA (Onpattro®) formulation for the treatment of polyneuropathies induced by hereditary transthyretin amyloidosis and the FDA approval of two Covid-19 LNP-mRNA vaccine formulations in 2020 that were optimized for mRNA delivery.[25-29] To achieve efficient transfection, disruption of the LNP structure and the endosomal membrane is crucial for sufficient RNA delivery into the cytoplasm.[30] However, in this process the majority (≥98%) of RNA molecules delivered with LNP systems remain trapped inside the endo/lysosome, leading to degradation or efflux out of the cell.[31,32] Thus there is room to

improve the therapeutic efficacy of mRNA therapies if cytoplasm delivery could be enhanced.

Fusion of lipid membranes occurs in many biological processes, including organelle inheritance in cell growth and division, chemical synaptic transmission in the nervous system, and the modulation of synaptic strength in memory and learning evolvement.[33] These fusion events are controlled by complementary specialized SNARE protein subunits, which form so-called coiled-coil complexes driving the docking of transport vesicles to the target plasma membrane resulting in membrane fusion and cargo delivery (*e.g.* in neuronal exocytosis).[34] Coiled-coil induced membrane fusion independent of endocytosis could be beneficial to facilitate endo/lysosome escape and boost the transfection efficiency of mRNA in cells.

In Chapter 2 we modified LNPs encapsulating mRNA with a heterodimeric coiled-coil peptide (denoted E4/K4) which induced prompt and highly efficient transfection and in this chapter mRNA delivery to iPSC-cardiomyocytes was studied. The Onpattro LNP formulation was modified with lipopeptide CPE4 (denoted as MC3-CPE4) and enhanced transfection of genetic cargo was observed following a 1-step incubation protocol of cells with a mixture of MC3-CPE4 and the complimentary lipopeptide CPK4. When this approach was used with the Covid-19 vaccine LNP-mRNA formulations, significantly enhanced mRNA expression was also obtained. In this study we apply coiled-coil peptide modified LNPs to transfect iPSC-CMs, resulting in a significant improvement of transfection (**Scheme 1**). These findings hold great promise for further *in vivo* research toward the development of efficient cardiomyocytes transfection and stimulation of cardiac repair and ultimately regeneration to rescue the ischemic myocardium.
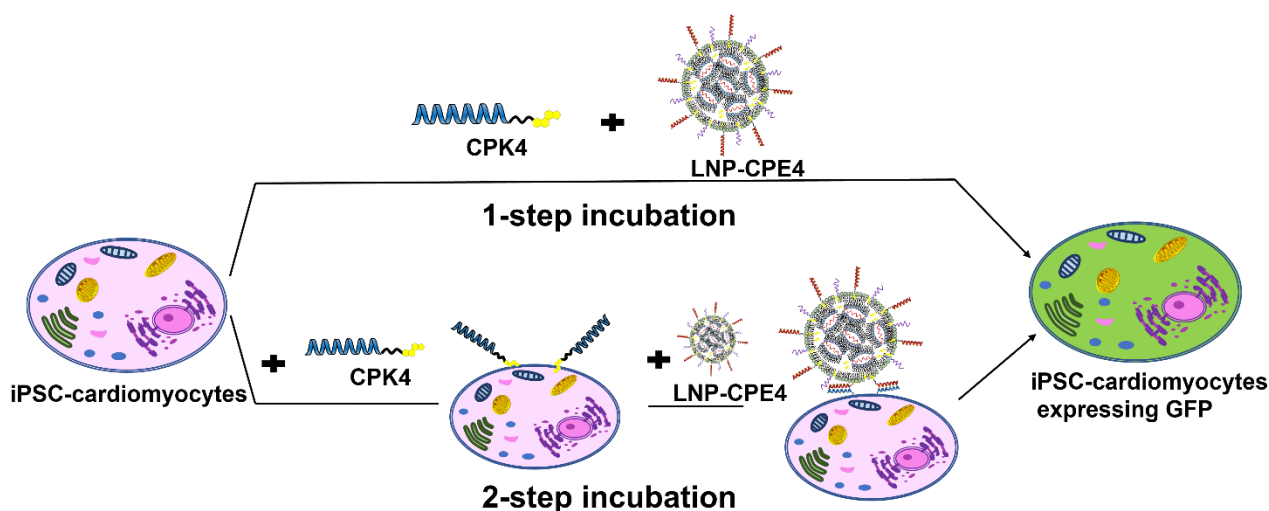
Scheme 1. *Schematic representation of fusogenic coiled-coil peptide modified lipid nanoparticles (LNPs) that induce efficient mRNA delivery within iPSC-cardiomyocytes using different delivery protocols.*
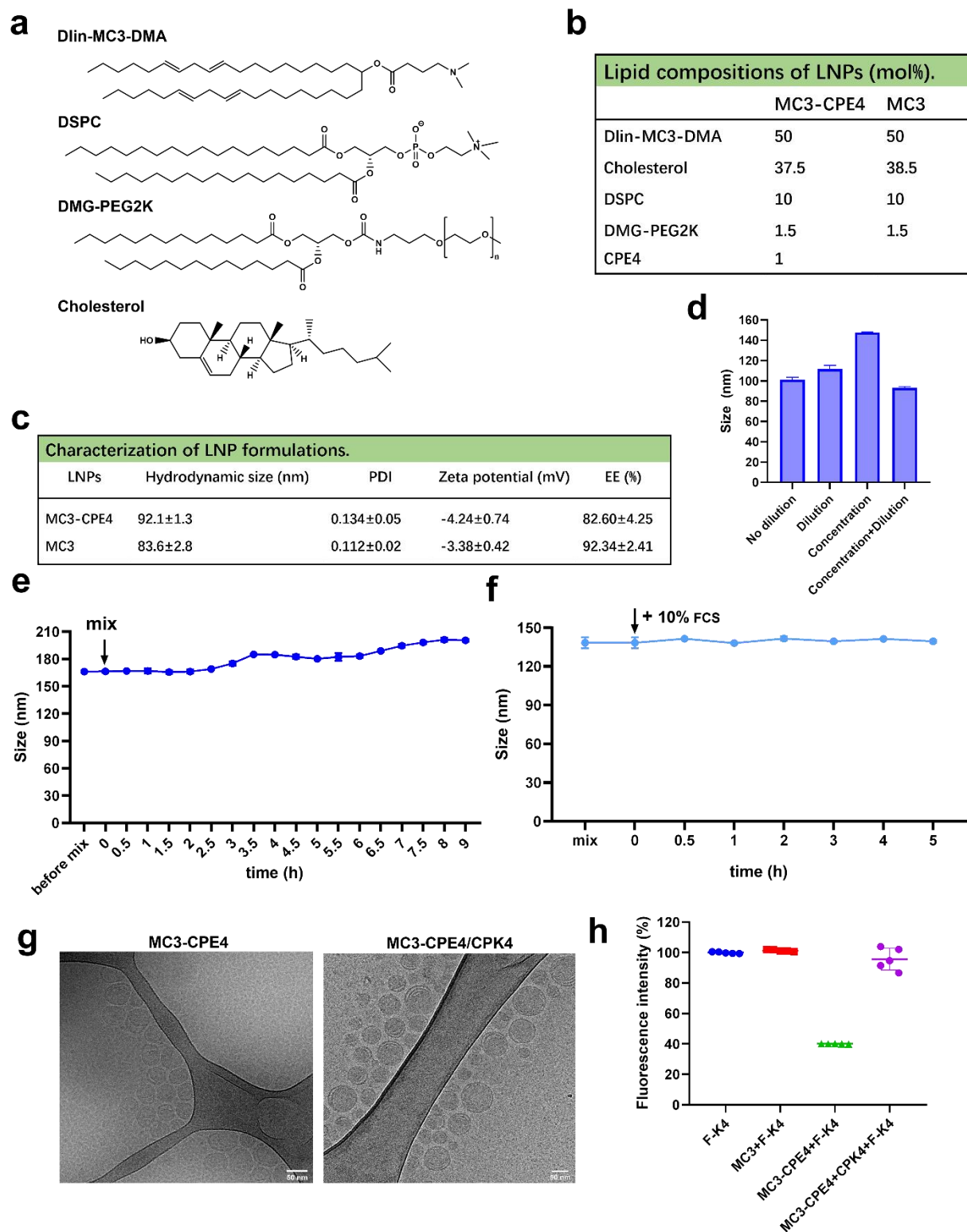
Results and discussion

LNP design, formulation, and characterization
The clinically approved LNP formulation Onpattro (short name MC3) was designed for potent

silencing of protein expression in cells by delivering siRNA (**Fig. 1a-b**).[35, 36] Two other LNP formulations with ionizable lipids either ALC0315 or SM102 were also studied (**SI Fig. 1a**). In this study, lipopeptide CPE4 (1 mol%) was added to the LNP formulations, resulting in CPE4-modified LNPs (**Fig. 1b, SI Fig. 1b**). After encapsulating EGFP-mRNA, the hydrodynamic diameter, polydispersities (PDI), zeta potential, and mRNA encapsulation efficiency of these LNPs was not changed by the addition of lipopeptide CPE4 (**Fig. 1c, SI Fig. 1b**). This showed that various clinically approved LNP formulations can be modified with lipidated coiled-coil peptides without altering the physicochemical characteristics.

In chapter 2 we showed that coiled-coil peptide modification of LNPs significantly improved the transfection efficiency in many cell lines *in vitro*. Here we studied whether these fusogenic peptides could be used to transfect cardiomyocytes. For *in vivo* applications, the intramyocardial injection volume of mice is very small (10 µL) requiring a high concentration of LNPs to obtain a sufficient mRNA dose. Dynamic light scattering measurements (DLS) revealed that the observed hydrodynamic diameter of the MC3-CPE4 was independent of concentration (**Fig. 1d**).

b. Lipid compositions of LNPs (mol%).

	MC3-CPE4	MC3
Dlin-MC3-DMA	50	50
Cholesterol	37.5	38.5
DSPC	10	10
DMG-PEG2K	1.5	1.5
CPE4	1	

c. Characterization of LNP formulations.

LNPs	Hydrodynamic size (nm)	PDI	Zeta potential (mV)	EE (%)
MC3-CPE4	92.1±1.3	0.134±0.05	-4.24±0.74	82.60±4.25
MC3	83.6±2.8	0.112±0.02	-3.38±0.42	92.34±2.41

Figure 1. Design and characterization of LNPs carrying EGFP-mRNA. (a) Structures of lipids used for the preparation of MC3-LNPs. **(b)** Lipid composition of LNPs. **(c)** Characterization of LNPs. **(d)** Hydrodynamic diameter of MC3-CPE4 as an indication for concentration and dilution. **(e)** Hydrodynamic diameter changes over time after mixing MC3-CPE4 with CPK4. **(f)** Hydrodynamic diameter changes over time of the mixture of MC3-CPE4 and CPK4 after 10% FCS addition. The nanoparticle diameter and PDI were monitored by DLS (mean ± s.d.,

n = 3). **(g)** Representative cryo-EM images of coiled-coil peptide modified MC3-CPE4 before and after mixing with the complimentary peptide. Scale bar is 50 nm. **(h)** Fluorescence intensity changes of fluorescein-labeled K4 peptide after addition to LNPs.

Nanoparticle characterizations of the 1-step incubation approach

Initially, we used a 2-step incubation protocol to deliver mRNA to cells, which requires the pretreatment of target cells before complementary LNPs are added. Cardiac mRNA delivery is usually achieved by direct intramyocardial injection of mRNA formulations in an open-chest surgery, and a shorter time of surgery will be beneficial for mouse survival.[20] Therefore a 1-step incubation protocol would be favorable. For this, we evaluated whether a 1-step incubation protocol was able to successfully transfect cells by premixing MC3-CPE4 and the complementary peptide CPK4 before mixing with cells. The hydrodynamic diameter change of this mixture was monitored by DLS as a function of time. After 2.5 h a slight increase in size was observed (**Fig. 1e**). Still, the overall diameter remained rather stable for a prolonged period of time and no massive aggregation was observed, which suggests that premixing does not negatively impact the colloidal stability of LNPs enabling a 1-step incubation protocol in future *in vivo* studies.

Next, the stability of the mixture MC3-CPE4 and CPK4 in the presence of 10% fetal calf serum (FCS) was studied. Again, no obvious size increase was observed (**Fig. 1f**). Cryogenic electron microscopy (cryo-EM) was applied to observe the morphology of MC3-CPE4 before and after mixing with the complimentary peptide CPK4 (**Fig. 1g**). No apparent changes in structure or aggregation was observed. Both amorphous and lamellar core structures of MC3-CPE4 were still present, whereas the core structure contained a mixture of amorphous, unilamellar, and polymorphic structures, as has been previously reported for mRNA containing LNPs.[37, 38]

LNP formulations consist of PEG chains (PEG2K), and mRNA delivery induced by coiled-coil peptide modified LNPs requires both coiled-coil peptides to be accessible, therefore to study whether CPE4 located on the surface of LNPs is still accessible to CPK4 even though the PEG chains are longer than the peptides, a fluorescence assay was used. Fluorescence intensity changes were monitored as an indication of binding affinity between peptides E and K after adding fluorescein-labeled K4 peptide (F-K4) to LNPs (**Fig. 1h**). Free F-K4 peptide served as a control, exhibiting 100% fluorescence intensity. As expected, when F-K4 was added to MC3, the fluorescence intensity was similar to free F-K4, demonstrating that free F-K4 failed to interact with the unmodified LNPs in the absence of CPE4. In contrast, when F-K4 was added to MC3-CPE4, the fluorescence intensity showed a significant reduction to 40%, indicating that F-K4 successfully binds to CPE4 at the LNP surface. When F-K4 was added to the mixture of MC3-CPE4 and CPK4, the fluorescence intensity was 96%, close to free F-K4, revealing that all CPE4 were already occupied by CPK4 via coiled-coil formation. This assay thus confirmed that the peptides are able to form coiled coils, even though the peptides are most likely buried in a PEG brush at the surface of LNPs.
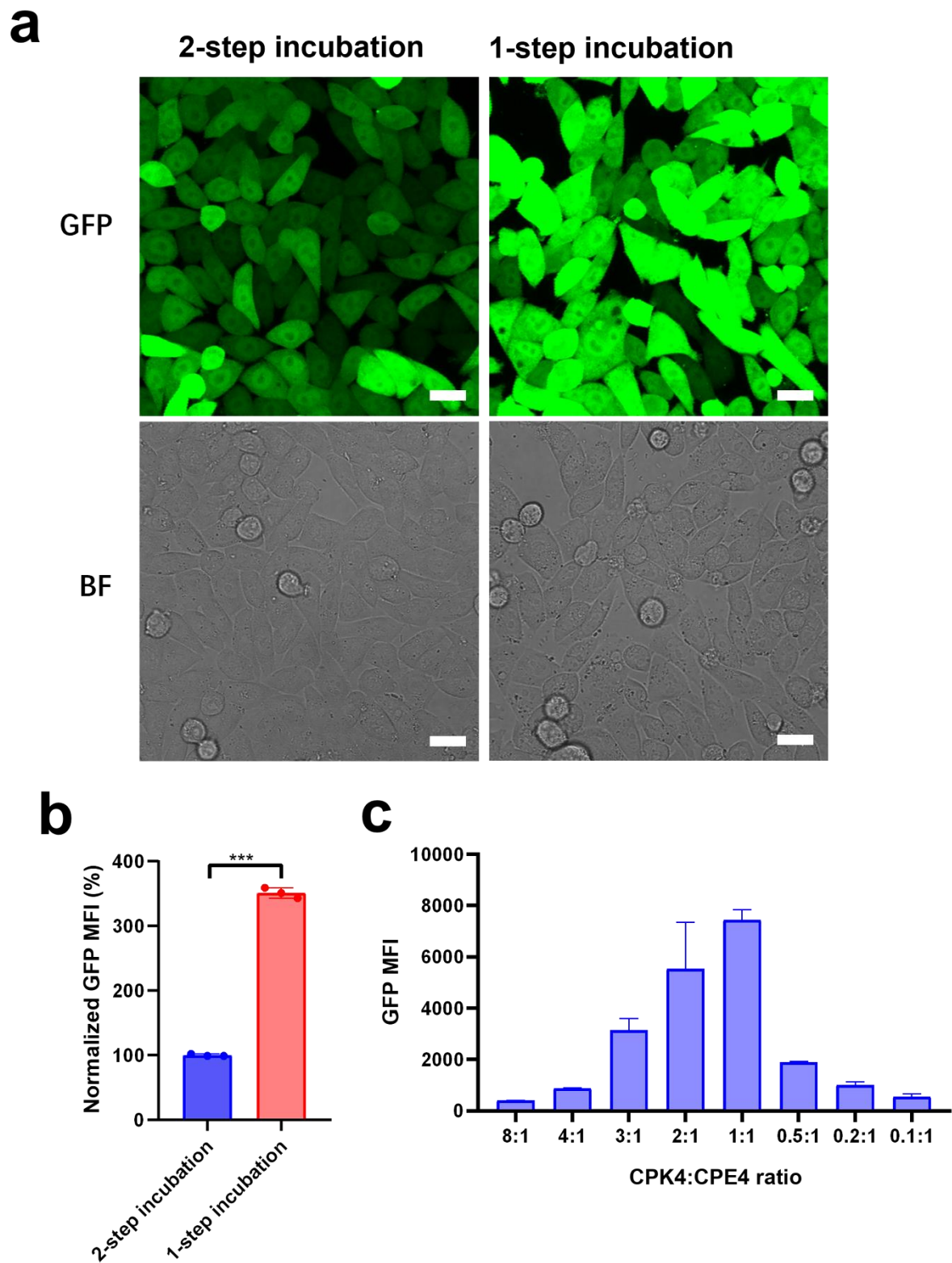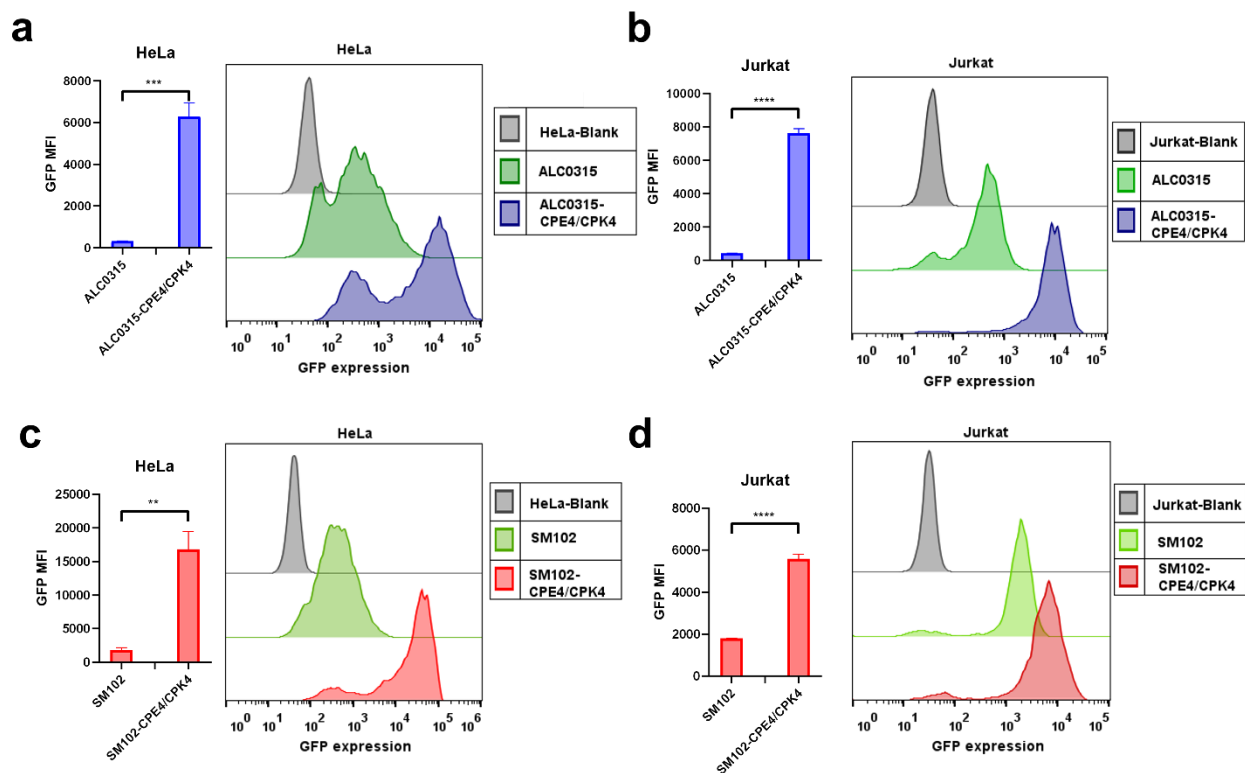
Figure 2. Transfection efficiency evaluation of different incubation protocols with HeLa cells. (a) Confocal microscopy images of mRNA transfection following different incubation protocols. 2-step incubation: cells were pretreated with CPK4 (10 μM, 200 μL) for 2 h, then the medium was removed and MC3-CPE4 was added (1 μg/mL,

200 µL) and incubated for 24 h before imaging. 1-step incubation: medium containing CPK4 and MC3-CPE4 (1 µg/mL, 200 µL, final concentration of CPK4:CPE4=1:1) was added to the cells and incubated for 24 h before imaging. GFP: green fluorescent protein; BF: bright field; scale bar is 20 µm. **(b)** Flow cytometry measurements of GFP expression intensity (GFP MFI) of the two protocols. MFI of the 1-step incubation was normalized to the 2-step incubation. Unpaired student t-test was used to determine the significance of data comparisons (****, $P < 0.0001$, ***, $P < 0.001$, **, $P < 0.01$, *, $P < 0.05$, ns, no significant difference). In all panels, error bars represent s.d. (n=3). **(c)** Transfection efficiency of CPK4:CPE4 ratio optimization following the 1-step incubation protocol. All LNPs were formulated using MC3 lipids and encapsulated with EGFP-mRNA. The EGFP-mRNA concentration encapsulated in MC3-CPE4 was 1 µg/mL.

Transfection performance of different incubation protocols

Next, we compared the transfection efficiencies between the 1-step and the 2-step incubation protocols as the former will be beneficial for future *in vivo* studies. Surprisingly, the 1-step incubation induced the strongest GFP expression (**Fig. 2a**). Flow cytometry analysis confirmed that the 1-step incubation indeed resulted in a higher mRNA transfection efficiency compared to the 2-step incubation, the former resulting in a 3-fold stronger GFP expression level (**Fig. 2b**). This experiment demonstrated that the 1-step incubation protocol is efficient and enables the future use in *in vivo* studies.

Next, we optimized the CPK4:CPE4 ratio for the 1-step incubation protocol. The mRNA concentration of MC3-CPE4 was kept constant while CPK4 and MC3-CPE4 were used at different final ratios. The highest GFP expression was obtained when an equimolar ratio of CPK4:CPE4 was used (**Fig. 2c**). In summary, the 1-step incubation protocol is a viable delivery approach, and the 1:1 ratio of CPK4:CPE4 is the most optimal ratio to achieve maximal transfection efficiency enhancement.
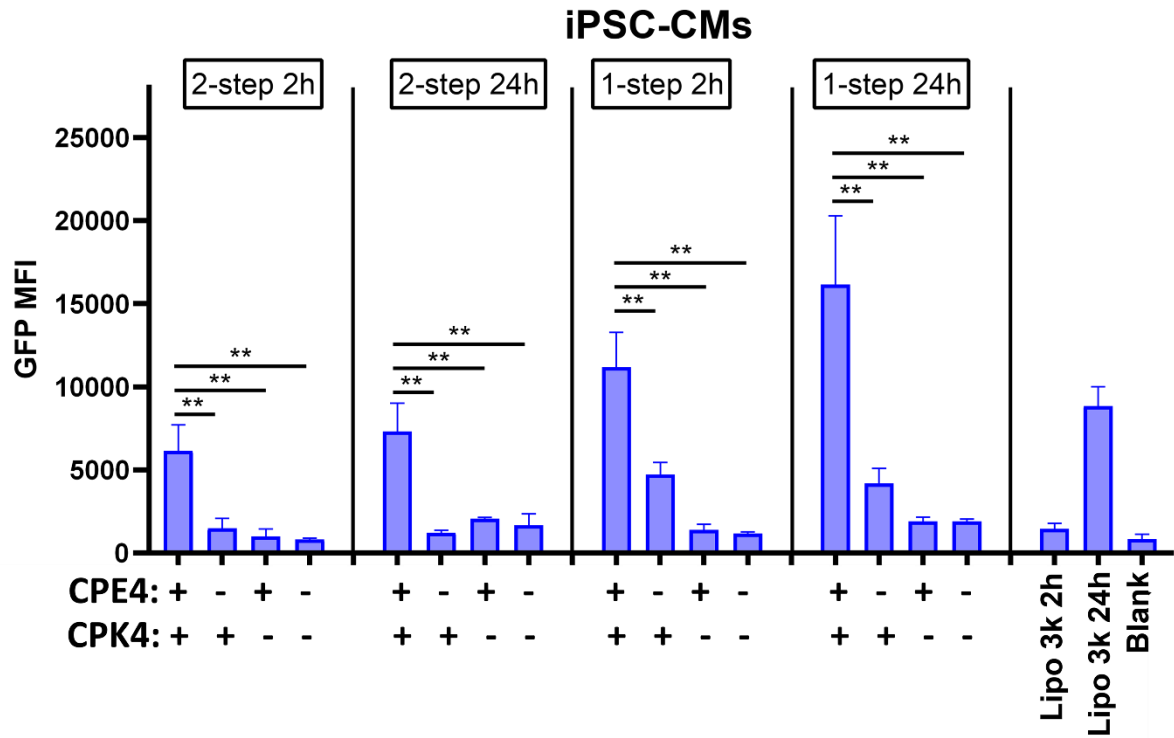
Figure 3. Transfection efficiency using fusogenic coiled-coil modified LNPs is independent of lipid composition. (a-b) The GFP expression fluorescence intensity (GFP MFI) of LNPs after encapsulating EGFP-mRNA (1 µg/mL, 24 h) within HeLa and Jurkat cells using ALC0315 from Pfizer/BioNTech Covid-19 LNP-mRNA formulation following the 1-step incubation protocol and incubating for 24 h. **(c-d)** The GFP expression fluorescence intensity (GFP MFI) of LNPs after encapsulating EGFP-mRNA (1 µg/mL, 24 h) within HeLa and Jurkat cells using SM102 from Moderna Covid-19 LNP-mRNA formulation following the 1-step incubation protocol and incubating for 24 h. Unpaired student t-test was used to determine the significance of data comparisons (****, $P < 0.0001$, ***, $P < 0.001$, **, $P < 0.01$, *, $P < 0.05$, ns, no significant difference). In all panels, error bars represent mean $\pm$ s.d. (n=3).

Transfection performance with other ionizable lipids

LNP formulations contain ionizable lipids that condense the genetic cargo and once inside the cell will influence the endosomal escape affecting the transfection performance.[39, 40] Coiled-coil peptide modified LNPs using MC3 as the ionizable lipid showed enhanced mRNA transfection. Now we wondered whether this enhancement of transfection efficiency could be achieved using other ionizable lipids (*i.e.* ALC0315 and SM102 from two Covid-19 LNP-mRNA vaccine formulations).[26, 28] Improved GFP expression was again observed with the introduction of coiled-coil peptides to these LNP formulations when using the 1-step incubation protocol (**Fig. 3a-d**). Thus enhanced mRNA transfection was not only observed in the Onpattro LNP formulation but also in other clinically approved LNPs when using the fusogenic coiled-coil peptides.
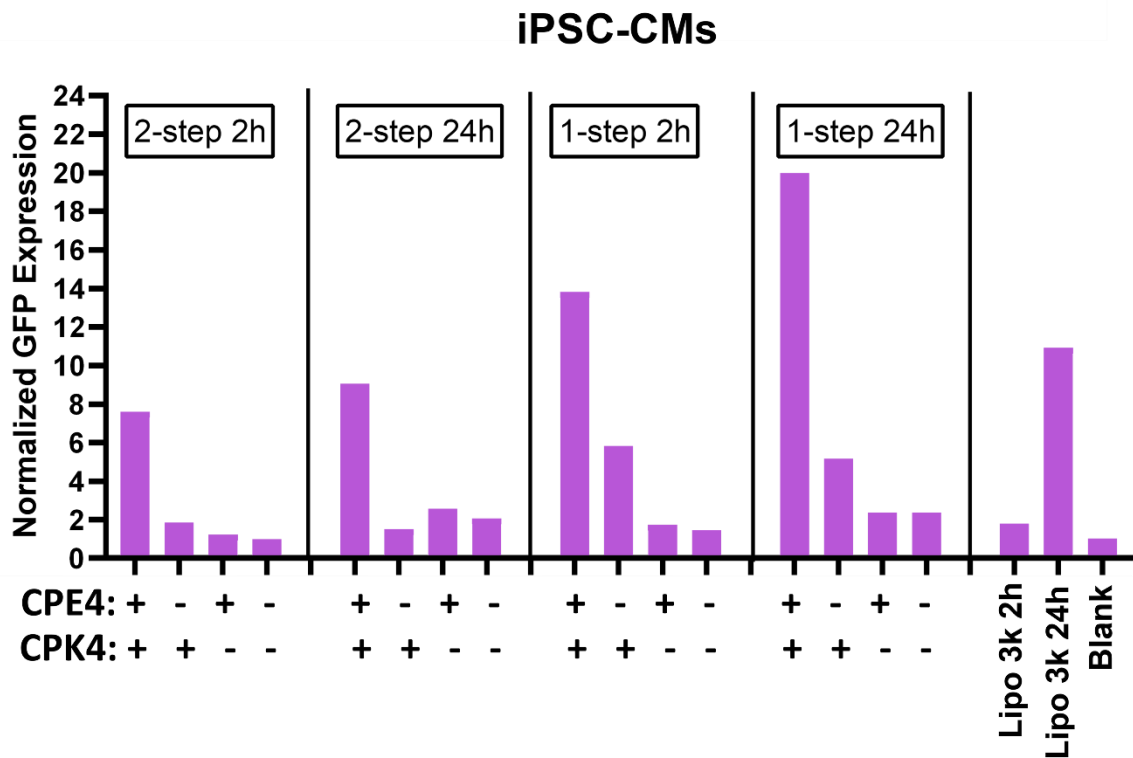
Figure 4. Transfection efficiency of the fusogenic coiled-coil modified LNPs using MC3 in iPSC-CMs *in vitro*. (a) The GFP expression fluorescence intensity (GFP MFI) of LNPs with iPSC-CMs was monitored by flow cytometry. (b) The GFP expression intensity normalized to MC3 (2-step incubation, 2 h). 2-step 2h: iPSC-CMs were pretreated with CPK4 (10 μM, 100 μL, 2 h), followed by incubation of MC3-CPE4 (2 μg/mL, 100 μL) for 2
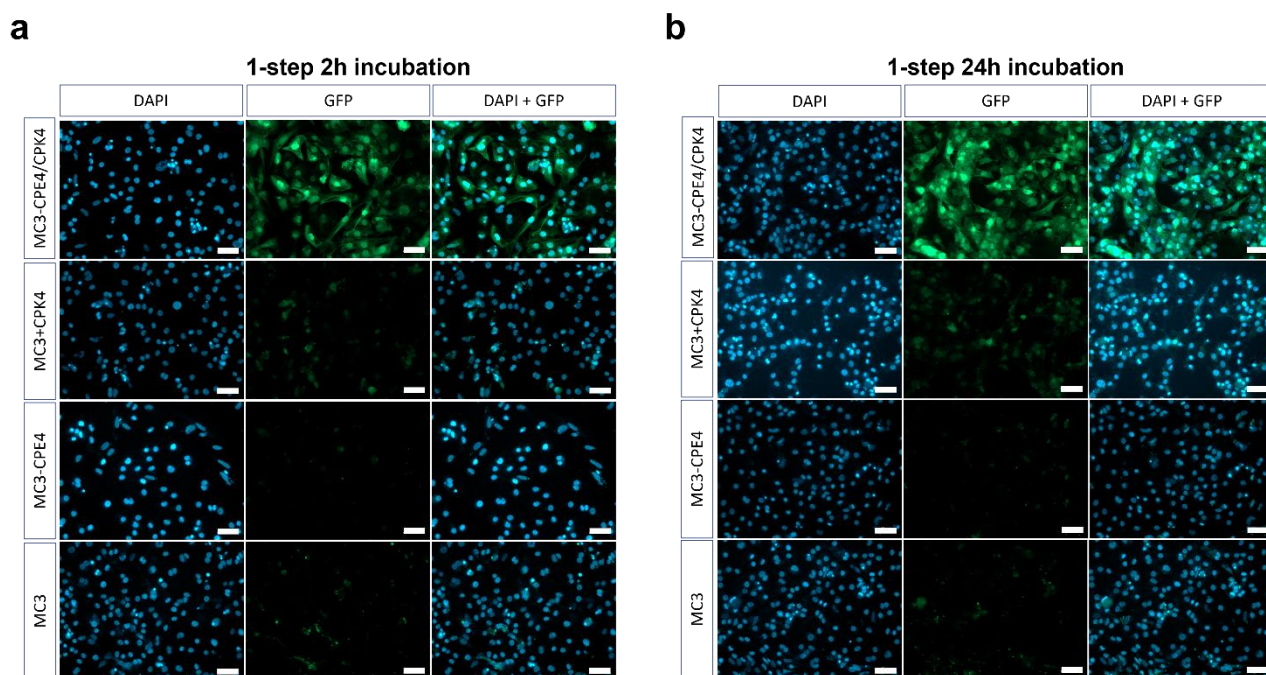
h, the supernatant was removed and cells were cultured for another 24 h before flow cytometry measurements. 1-step 2h incubation: a medium containing CPK4 and MC3-CPE4 (2 μg/mL, 100 μL, the final ratio of CPK4:CPE4=1:1) was added to the iPSC-CMs and incubated for 2 h, then the medium was removed and cells were cultured for another 24 h before flow cytometry measurements. For the 2-step 24h and 1-step 24h groups: iPSC-CMs were incubated with LNPs for 24 h before measuring, all other steps in the protocol remained the same. All LNPs were formulated using ionizable lipids MC3 and encapsulated with EGFP-mRNA. Unpaired student t-test was used to determine the significance of data comparisons (****, P < 0.0001, ***, P < 0.001, **, P < 0.01, *, P < 0.05, ns, no significant difference). In all panels, error bars represent s.d. (n=3).

Transfection efficiency in iPSC-CMs

Human-induced pluripotent stem cell-derived cardiomyocytes (iPSC-CMs) can produce relevant proteins found in adult human CMs, spontaneously contract, proliferate limitlessly, and differentiate into several cell types, therefore, they are often used for customized genome editing, cardiovascular disease modeling, and high-throughput drug screening.[41, 42] Here, we applied coiled-coil peptide modified MC3-LNPs to evaluate the *in vitro* transfection performance in iPSC-CMs and compared the transfection efficiency of different incubation protocols (2-step incubation *vs* 1-step incubation) and time (2 *vs* 24h). As expected, the introduction of fusogenic coiled-coil peptides to the LNPs induced highly efficient GFP transfection of iPSC-CMs for both incubation times. These transfection efficiencies were superior to unmodified LNPs and to the commercial transfection reagent Lipofectamine 3K (**Fig. 4a**). In line with previous experiments, the 1-step incubation protocol achieved better transfection performance than the 2-step incubation protocol, and increasing the incubation time from 2 to 24 h enhanced GFP expression.

Fusogenic coiled-coil peptides did significantly increase the transfection of iPSC-CMs; with up to a 19-fold increase when using the 1-step incubation protocol for 24 h (**Fig. 4b**), which is a significant transfection enhancement as compared to state-of-the-art LNPs.

Confocal microscopy imaging was applied to visualize GFP expression in iPSC-CMs following the 1-step incubation protocol. Intense GFP fluorescence was uniform in the majority of iPSC-CMs when fusogenic coiled-coil peptide modified LNPs were used to deliver mRNA, independent of incubation time. In contrast, weak GFP fluorescence was observed when unmodified LNPs were used to transfect the cells with mRNA (**Fig. 5a-b**). In summary, the use of fusogenic coiled-coil peptides to modify LNPs greatly enhanced the transfection of iPSC-CMs *in vitro*, holding great promise for cardiomyocyte transfection *in vivo*.

Figure 5. (a-b) Confocal images of the EGFP-mRNA transfection of LNPs following the 1-step incubation protocol. 1-step 2h incubation: a medium containing CPK4 and MC3-CPE4 (2 μg/mL, 500 μL, the final ratio of CPK4:CPE4=1:1) was added to the iPSC-CMs and incubated for 2 h, then the medium was removed and cells were cultured for another 24 h before imaging. 1-step 24h incubation: a medium containing CPK4 and MC3-CPE4 (2 μg/mL, 500 μL, the final ratio of CPK4:CPE4=1:1) was added to the iPSC-CMs and incubated for 24 h before imaging. All LNPs were formulated using MC3 ionizable lipids and encapsulated with EGFP-mRNA. Blue: DAPI; green: GFP, green fluorescent protein; scale bar is 50 μm.

Transfection efficiency evaluation on iPSC-CMs of LNPs using other ionizable lipids

The transfection performance of coiled-coil peptide modified LNPs in iPSC-CMs using ALC0315 and SM102 lipids was also evaluated using the 1-step incubation protocol. Flow cytometry analysis showed that all coiled-coil peptide modified LNPs greatly facilitated the cellular uptake of LNPs composing the ionizable lipids MC3, ALC0315, and SM102 (**Fig. 6a**). Consistent with the cellular uptake efficiency, the introduction of fusogenic coiled-coil peptides to LNPs produced significantly improved GFP expression compared to three naked LNPs (**Fig. 6b**). This further proved that enhanced mRNA transfection performance in iPSC-CMs could be achieved by various LNP formulations after the introduction of fusogenic coiled-coil peptides.
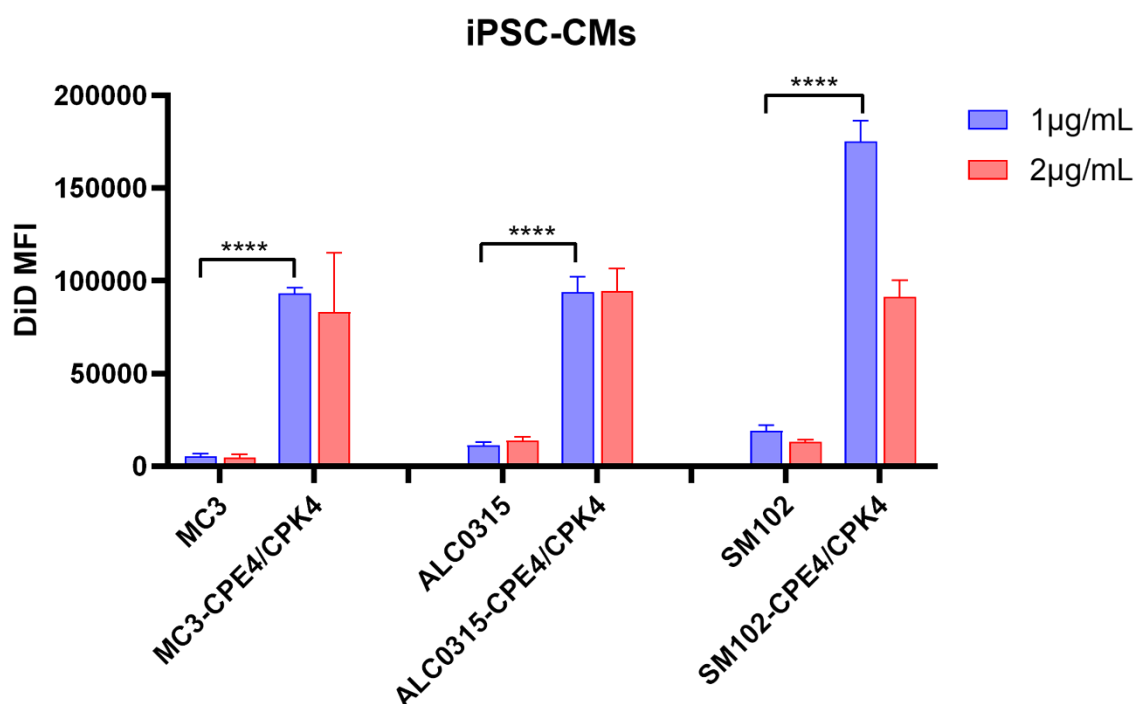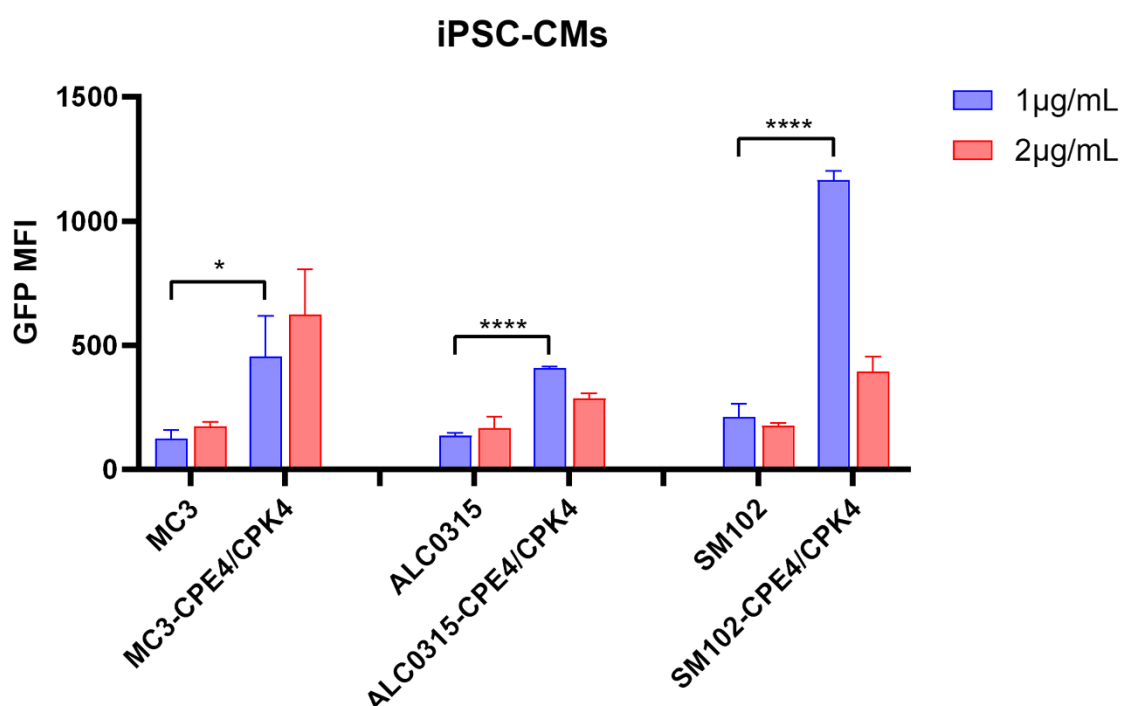
Figure 6. Transfection efficiency in iPSC-CMs of the coiled-coil modified LNPs using other ionizable lipids. **(a)** The cellular uptake efficiency of LNPs in iPSC-CMs using the 1-step incubation protocol and incubating for 24 h was measured by quantifying DiD fluorescence. 0.5 mol% of DiD was added to the lipids as a. **(b)** The GFP expression fluorescence intensity (GFP MFI) of LNPs with iPSC-CMs was measured by flow cytometry using the 1-step incubation protocol and incubating for 24 h. MC3 was used in the Onpattro LNP-siRNA formulation;

ALC0315 was used in the Pfizer/BioNTech Covid-19 LNP-mRNA vaccine formulation; SM102 was used in the Moderna Covid-19 LNP-mRNA vaccine formulation. All LNPs were encapsulated with EGFP-mRNA. Statistical significance was calculated by an unpaired student t-test on the 1 μg/mL data. (****, $P < 0.0001$, ***, $P < 0.001$, **, $P < 0.01$, *, $P < 0.05$, ns, no significant difference) In all panels, error bars represent mean $\pm$ s.d. (n=3).

Conclusions

Enhanced mRNA delivery into hard to transfect iPSC-CMs can be obtained by the introduction of fusogenic coiled coil peptides into state-of-the-art LNP formulations. In this study MC3-LNPs were modified with 1 mol% CPE4 lipopeptide, and cells were pretreated with the complementary lipopeptide CPK4. mRNA delivery was optimized by premixing CPK4 and MC3-CPE4 before adding this mixture to cells and this 1-step incubation protocol is compatible with future *in vivo* applications. Modification of LNPs with these lipopeptides did not change the physicochemical properties of these mRNA-containing nanoparticles. We also evaluated two Covid-19 LNP-mRNA vaccine formulations, which also showed enhanced transfection using the 1-step incubation protocol. The *in vitro* mRNA delivery in iPSC-CMs proved that the introduction of coiled-coil peptides into different LNP formulations greatly boosted mRNA transfection efficiency compared to LNPs without modification, resulting in higher GFP expression when encapsulating EGFP-mRNA. In summary, the introduction of fusogenic coiled-coil peptides to LNPs could potentially lead to the enhanced mRNA delivery in future *in vivo* cardiomyocyte research, which holds great promise for the development of a myocardium regenerative therapy after injury to prevent or treat heart failure by carrying a functional mRNA.

Methods

Chemicals and materials

Lipopeptides CPE4 and CPK4 were synthesized as described in Chapter 2 (**SI Fig. 1a**). 1,2-distearoyl-*sn*-glycero-3-phosphocholine (DSPC), 1,2-dimyristoyl-*rac*-glycero-3-methoxypolyethylene glycol-2000 (DMG-PEG2K) were purchased from Avanti Polar Lipids, DLin-MC3-DMA was purchased from Biorbyt company (Cambridge, England), cholesterol was purchased from Sigma-Aldrich. Triton™ X-100 was purchased from Acros Organics. 100k MWCO centrifugal filters (Amicon® Ultra, Merck) were purchased from Sigma. 1,1-dioctadecyl-3,3,3,3-tetramethylindodicarbocyanine (DiD), QuantiT™ RiboGreen® RNA Assay Kit was purchased from Life Technologies. Clean cap EGFP-mRNA was purchased from Trilink biotechnology. The ionizable lipids ALC0315 and SM102 were synthesized according to the literature (**SI Fig. 1a**).[39, 43]

HeLa and Jurkat cell lines purchased from ATCC were cultured according to ATCC guidelines. The DMEM and RPMI-1640 growth medium (Sigma Aldrich) containing sodium bicarbonate, without sodium pyruvate and HEPES, was supplemented with 10% fetal bovine serum (Sigma), 1% L-glutamine (Thermo Fisher Scientific) and 1% penicillin/streptomycin (Thermo Fisher Scientific), at 37 °C in the presence of 5% CO_2. HeLa was cultured with DMEM medium, Jurkat was cultured with RPMI-1640 medium. iPSC-CMs were cultured with RPMI/B27 medium (Thermo Fisher Scientific). Maturation media of iPSC-CMs was composed of DMEM without glucose (Thermo Fisher Scientific) supplemented with 3 mM glucose (Sigma Aldrich), 10 mM L-lactate (Sigma Aldrich), 5 mg/ml Vitamin B12 (Sigma Aldrich), 0.82 mM Biotin (Sigma Aldrich), 5 mM Creatine monohydrate (Sigma Aldrich), 2 mM Taurine (Sigma Aldrich), 2mM L-carnitine (Sigma Aldrich), 0.5 mM Ascorbic acid (Sigma Aldrich), 1x NEAA (Thermo Fisher Scientific), 0.5 % (w/v) Albumax (Thermo Fisher Scientific), 1x B27 and 1% KOSR (Thermo Fisher Scientific).

Lipid nanoparticle formulation and characterization

Stock solutions of lipids and lipopeptides in chloroform:methanol (1:1, v/v) were mixed in a vial at the desired molar ratios, the solvents were evaporated under a nitrogen flow and residual solvent was removed *in vacuo* for at least 30 minutes. The lipid film was dissolved in absolute ethanol and used for the assembly ([total lipid] = 1 μmol, N/P=16). EGFP-mRNA was diluted in 50 mM RNase free citrate buffer (pH = 4). The solutions were loaded into two separate syringes and connected to a T-junction microfluidic mixer. The solutions were mixed in a 3:1 flow ratio of nucleic acid against lipids (1.5 mL/min for mRNA solution, 0.5 mL/min for lipids solution). After mixing, the solution was directly loaded into a 20 kDa MWCO dialysis cassette (Slide-A-Lyzer™, Thermo Scientific) and dialyzed against 1X PBS overnight. mRNA encapsulation efficiency and mRNA concentrations were determined by a Quant-iT™ RiboGreen™ RNA Assay Kit.

All LNPs encapsulating EGFP-mRNA for transfection evaluation in HeLa, Jurkat, and iPSC-CMs cells were made in the same way. 0.5 mol% DiD was added to the lipids to prepare DiD-labeled LNPs for the quantification of LNP uptake on iPSC-CMs.

The hydrodynamic diameter, polydispersities, and zeta potentials of LNPs were measured using a Malvern zetasizer Nano ZS (DLS, Malvern).

MC3-CPE4 were concentrated using 100 kDa MWCO centrifugal filters, centrifuged at 4℃, 5000 RCF for 1-2 h. Adjustment and dilution of LNPs were done with 1X PBS. The hydrodynamic diameter changes over time after premixing CPK4 and MC3-CPE4 were monitored by the DLS measurements with the ratio of CPK4:CPE4=1:1. The serum stability was tested by measuring the hydrodynamic diameter changes of the mixture of CPK4 and MC3-CPE4 (CPK4:CPE4=1:1) after adding 10% FCS.

The morphology of LNPs was analyzed by cryogenic transmission electron microscopy (cryo-EM). Vitrification of concentrated (~10 mM) LNPs was performed using a Leica EM GP operating at 21 °C and 95% room humidity (RH). Sample suspensions were placed on glow discharged 100 μm lacey carbon films supported by 200 mesh copper grids (Electron Microscopy Sciences). Optimal results were achieved using a 60-second pre-blot and a 1-second blot time. After vitrification, sample grids were maintained below -170 °C, and imaging was performed on a Tecnai T12 (ThermoFisher) with a biotwin lens and LaB6 filament operating at 120 keV equipped with an Eagle 4K×4K CCD camera (ThermoFisher). Images were acquired at a nominal underfocus of -2 to -3 μm (49,000× magnification) with an electron dose of ~2000 e/nm2. For cryo-EM imaging, CPK4 was added to the MC3-CPE4 with the ratio of CPK4:CPE4=1:1, then incubated for 1 h before imaging.

For the coiled-coil peptide CPK4 binding assay, fluorescein-labeled K4 peptide was added to the MC3-CPE4 (final ratio of CPK4:CPE4=1:1) and incubated at RT for 1-2 h, followed by centrifugation (Amicon Ultra-0.5 Centrifugal Filter Unit, 5000 RCF, 30 min). The solution in the lower tube was collected the and fluorescence intensity was quantified by Tecan plate reader (excitation wavelength: 480 nm; emission wavelength: 520 nm). The fluorescence intensity was normalized to free fluorescein-K4.

Transfection of HeLa cells
HeLa cells were seeded in an 8-well confocal plate at a density of $5*10^4$ cells/well. 2-step incubation protocol: HeLa cells were pretreated with CPK4 (10 μM, 200 μL) for 2 h, then the medium was removed and MC3-CPE4 (1 μg/mL, 200 μL) was added and incubated for 24 h before imaging. 1-step incubation protocol: a medium containing CPK4 and MC3-CPE4 (EGFP-mRNA=1 μg/mL, CPE4=2.5 μM, CPK4=2.5 μM, 200μL, the final ratio of CPK4:CPE4=1:1) was added to the cells and incubated for 24 h before imaging. Flow cytometry measurements of the two incubation protocols were carried out with cells seeded in 96-well plates at a density of $1*10^4$ cells/well, then the same incubation protocols were followed. The mean fluorescence intensity of GFP expression for the 1-step incubation was normalized to the 2-step incubation.

To determine the optimal CPK4:CPE4 ratio for mRNA transfection, HeLa cells were seeded in a 96-well plate at a density of $1*10^4$ cells/well. The concentration of EGFP-mRNA added to cells was 1 μg/mL. CPK4 and MC3-CPE4 with different final ratios of CPK4:CPE4 (CPK4:CPE4=8:1, 4:1, 3:1, 2:1, 1:1, 0.5:1, 0.2:1, 0.1:1) were added together to cells and incubated for 24 h before analysis by flow cytometry.

For the transfection evaluation of LNP formulations composing other ionizable lipids ALC0315 and SM102 using the 1-step incubation protocol, HeLa and Jurkat cells were seeded in a 96-well plate with a density of $1*10^4$ cells/well, then ALC0315, SM102 (EGFP-mRNA=1 μg/mL, 100 μL),

ALC0315-CPE4/CPK4, and SM102-CPE4/CPK4 (EGFP-mRNA=1 μg/mL, 100 μL, CPK4:CPE4=1:1) were added to the cells and incubated for 24 h before flow cytometry measurements.

Transfection evaluation of iPSC-CMs

iPSC-CMs were seeded at the density of $1*10^5$ cells/well in a 96-well plate for flow cytometry measurements. 2-step incubation 2h protocol: iPSC-CMs cells were pretreated with CPK4 (10 μM, 100 μL) for 2 h, then the medium was removed and MC3-CPE4 (2 μg/mL, 100 μL) was incubated for 2 h, the supernatant was removed and cells were cultured for another 24 h before flow cytometry measurements. 1-step incubation 2h protocol: a medium containing CPK4 and LNPs (2 μg/mL, 100 μL, the final ratio of CPK4:CPE4=1:1) was added to the iPSC-CMs and incubated for 2 h, then the medium was removed and cells were cultured for another 24 h before FACs measurements. 2-step incubation-24h and 1-step incubation-24h: The same incubation protocols were followed but iPSC-CMs were incubated with LNPs for 24 h before measuring. All LNPs were formulated using ionizable lipids MC3 and encapsulated with EGFP-mRNA.

For confocal imaging, iPSC-CMs were seeded at the density of $5*10^5$ cells/well in a 24-well confocal plate. 1-step 2h incubation group: a medium containing CPK4 and MC3-CPE4 (2 μg/mL, 500 μL, the final ratio of CPK4:CPE4=1:1) was added to the iPSC-CMs cells, incubated for 2 h, then the supernatant was removed and refreshed with new medium and cells were cultured for another 24 h before imaging. LNPs were incubated with iPSC-CMs for 24 h in the group of 1-step 24h incubation.

The transfection of iPSC-CMs of LNP formulations composing other ionizable lipids ALC0315 and SM102 was carried out by following the 1-step incubation protocol. Cellular uptake efficiency was measured by quantifying the DiD fluorescence of LNPs (0.5 mol% DiD was added to the lipids) by flow cytometry measurements. The fluorescence intensity of GFP expression was measured to compare the transfection efficiency.

Statistical analysis

All experiments were performed at least in triplicate (n=3) unless specified otherwise, and the significance was determined using an unpaired student t-test (Graphpad Prism) for all comparisons. ****, $P < 0.0001$, ***, $P < 0.001$, **, $P < 0.01$, *, $P < 0.05$, ns, no significant difference.

References

1. Bui, A. L.; Horwich, T. B.; Fonarow, G. C., Epidemiology and risk profile of heart failure. *Nature Reviews Cardiology* **2011,** *8* (1), 30-41.
2. Zoni-Berisso, M.; Lercari, F.; Carazza, T.; Domenicucci, S., Epidemiology of atrial fibrillation: European perspective. *Clinical epidemiology* **2014,** *6*, 213.
3. Groenewegen, A.; Rutten, F. H.; Mosterd, A.; Hoes, A. W., Epidemiology of heart failure. *European Journal of Heart Failure* **2020,** *22* (8), 1342-1356.
4. Senyo, S. E.; Steinhauser, M. L.; Pizzimenti, C. L.; Yang, V. K.; Cai, L.; Wang, M.; Wu, T.-D.; Guerquin-Kern, J.-L.; Lechene, C. P.; Lee, R. T., Mammalian heart renewal by pre-existing cardiomyocytes. *Nature* **2013,** *493* (7432), 433-436.
5. Whelan, R. S.; Kaplinskiy, V.; Kitsis, R. N., Cell Death in the Pathogenesis of Heart Disease: Mechanisms

and Significance. *Annual Review of Physiology* **2010,** *72* (1), 19-44.

6.   Yang, Q.;   Fang, J.;   Lei, Z.;   Sluijter, J. P. G.; Schiffelers, R., Repairing the heart: State-of the art delivery strategies for biological therapeutics. *Advanced Drug Delivery Reviews* **2020,** *160*, 1-18.

7.   Laflamme, M. A.; Murry, C. E., Heart regeneration. *Nature* **2011,** *473* (7347), 326-335.

8.   Smith, A. S. T.;   Macadangdang, J.;   Leung, W.;   Laflamme, M. A.; Kim, D.-H., Human iPSC-derived cardiomyocytes and tissue engineering strategies for disease modeling and drug screening. *Biotechnology Advances* **2017,** *35* (1), 77-94.

9.   Shiba, Y.;   Gomibuchi, T.;   Seto, T.;   Wada, Y.;   Ichimura, H.;   Tanaka, Y.;   Ogasawara, T.;   Okada, K.;   Shiba, N.;   Sakamoto, K.;   Ido, D.;   Shiina, T.;   Ohkura, M.;   Nakai, J.;   Uno, N.;   Kazuki, Y.;   Oshimura, M.;   Minami, I.; Ikeda, U., Allogeneic transplantation of iPS cell-derived cardiomyocytes regenerates primate hearts. *Nature* **2016,** *538* (7625), 388-391.

10.   Lalit, P. A.;   Hei, D. J.;   Raval, A. N.; Kamp, T. J., Induced Pluripotent Stem Cells for Post–Myocardial Infarction Repair. *Circulation Research* **2014,** *114* (8), 1328-1345.

11.   Lian, X.;   Hsiao, C.;   Wilson, G.;   Zhu, K.;   Hazeltine, L. B.;   Azarin, S. M.;   Raval, K. K.;   Zhang, J.;   Kamp, T. J.; Palecek, S. P., Robust cardiomyocyte differentiation from human pluripotent stem cells via temporal modulation of canonical Wnt signaling. *Proceedings of the National Academy of Sciences* **2012,** *109* (27), E1848-E1857.

12.   Paige, Sharon L.;   Thomas, S.;   Stoick-Cooper, Cristi L.;   Wang, H.;   Maves, L.;   Sandstrom, R.;   Pabon, L.;   Reinecke, H.;   Pratt, G.;   Keller, G.;   Moon, Randall T.;   Stamatoyannopoulos, J.; Murry, Charles E., A Temporal Chromatin Signature in Human Embryonic Stem Cells Identifies Regulators of Cardiac Development. *Cell* **2012,** *151* (1), 221-232.

13.   Park, H.;   Larson, B. L.;   Kolewe, M. E.;   Vunjak-Novakovic, G.; Freed, L. E., Biomimetic scaffold combined with electrical stimulation and growth factor promotes tissue engineered cardiac development. *Experimental Cell Research* **2014,** *321* (2), 297-306.

14.   Lin, Z.;   von Gise, A.;   Zhou, P.;   Gu, F.;   Ma, Q.;   Jiang, J.;   Yau, A. L.;   Buck, J. N.;   Gouin, K. A.;   van Gorp, P. R. R.;   Zhou, B.;   Chen, J.;   Seidman, J. G.;   Wang, D.-Z.; Pu, W. T., Cardiac-Specific YAP Activation Improves Cardiac Function and Survival in an Experimental Murine MI Model. *Circulation Research* **2014,** *115* (3), 354-363.

15.   Tao, Z.;   Chen, B.;   Tan, X.;   Zhao, Y.;   Wang, L.;   Zhu, T.;   Cao, K.;   Yang, Z.;   Kan, Y. W.; Su, H., Coexpression of VEGF and angiopoietin-1 promotes angiogenesis and cardiomyocyte proliferation reduces apoptosis in porcine myocardial infarction (MI) heart. *Proceedings of the National Academy of Sciences* **2011,** *108* (5), 2064-2069.

16.   Zangi, L.;   Lui, K. O.;   von Gise, A.;   Ma, Q.;   Ebina, W.;   Ptaszek, L. M.;   Später, D.;   Xu, H.;   Tabebordbar, M.;   Gorbatov, R.;   Sena, B.;   Nahrendorf, M.;   Briscoe, D. M.;   Li, R. A.;   Wagers, A. J.;   Rossi, D. J.;   Pu, W. T.; Chien, K. R., Modified mRNA directs the fate of heart progenitor cells and induces vascular regeneration after myocardial infarction. *Nature Biotechnology* **2013,** *31* (10), 898-907.

17.   Gabisonia, K.;   Prosdocimo, G.;   Aquaro, G. D.;   Carlucci, L.;   Zentilin, L.;   Secco, I.;   Ali, H.;   Braga, L.;   Gorgodze, N.;   Bernini, F.;   Burchielli, S.;   Collesi, C.;   Zandona, L.;   Sinagra, G.;   Piacenti, M.;   Zacchigna, S.;   Bussani, R.;   Recchia, F. A.; Giacca, M., MicroRNA therapy stimulates uncontrolled cardiac repair after myocardial infarction in pigs. *Nature* **2019,** *569* (7756), 418-422.

18.   Su, H.;   Joho, S.;   Huang, Y.;   Barcena, A.;   Arakawa-Hoyt, J.;   Grossman, W.; Kan, Y. W., Adeno-associated viral vector delivers cardiac-specific and hypoxia-inducible VEGF expression in ischemic mouse hearts. *Proceedings of the National Academy of Sciences* **2004,** *101* (46), 16280-16285.

19.   Engel, F. B.;   Hsieh, P. C.;   Lee, R. T.; Keating, M. T., FGF1/p38 MAP kinase inhibitor therapy induces cardiomyocyte mitosis, reduces scarring, and rescues function after myocardial infarction. *Proceedings of the*

National Academy of Sciences **2006,** *103* (42), 15546-15551.

20. Sultana, N.; Magadum, A.; Hadas, Y.; Kondrat, J.; Singh, N.; Youssef, E.; Calderon, D.; Chepurko, E.; Dubois, N.; Hajjar, R. J.; Zangi, L., Optimizing Cardiac Delivery of Modified mRNA. *Molecular Therapy* **2017,** *25* (6), 1306-1315.

21. Kaur, K.; Zangi, L., Modified mRNA as a Therapeutic Tool for the Heart. *Cardiovascular Drugs and Therapy* **2020,** *34* (6), 871-880.

22. Hadas, Y.; Katz, M. G.; Bridges, C. R.; Zangi, L., Modified mRNA as a therapeutic tool to induce cardiac regeneration in ischemic heart disease. *WIREs Systems Biology and Medicine* **2017,** *9* (1), e1367.

23. Delivering the promise of RNA therapeutics. *Nature Medicine* **2019,** *25* (9), 1321-1321.

24. Yin, H.; Kanasty, R. L.; Eltoukhy, A. A.; Vegas, A. J.; Dorkin, J. R.; Anderson, D. G., Non-viral vectors for gene-based therapy. *Nature Reviews Genetics* **2014,** *15* (8), 541-555.

25. Kulkarni, J. A.; Witzigmann, D.; Thomson, S. B.; Chen, S.; Leavitt, B. R.; Cullis, P. R.; van der Meel, R., The current landscape of nucleic acid therapeutics. *Nature Nanotechnology* **2021,** *16* (6), 630-643.

26. Verbeke, R.; Lentacker, I.; De Smedt, S. C.; Dewitte, H., The dawn of mRNA vaccines: The COVID-19 case. *Journal of Controlled Release* **2021,** *333*, 511-520.

27. Polack, F. P.; Thomas, S. J.; Kitchin, N.; Absalon, J.; Gurtman, A.; Lockhart, S.; Perez, J. L.; Pérez Marc, G.; Moreira, E. D.; Zerbini, C.; Bailey, R.; Swanson, K. A.; Roychoudhury, S.; Koury, K.; Li, P.; Kalina, W. V.; Cooper, D.; Frenck, R. W.; Hammitt, L. L.; Türeci, Ö.; Nell, H.; Schaefer, A.; Ünal, S.; Tresnan, D. B.; Mather, S.; Dormitzer, P. R.; Şahin, U.; Jansen, K. U.; Gruber, W. C., Safety and Efficacy of the BNT162b2 mRNA Covid-19 Vaccine. *New England Journal of Medicine* **2020,** *383* (27), 2603-2615.

28. Shin, M. D.; Shukla, S.; Chung, Y. H.; Beiss, V.; Chan, S. K.; Ortega-Rivera, O. A.; Wirth, D. M.; Chen, A.; Sack, M.; Pokorski, J. K.; Steinmetz, N. F., COVID-19 vaccine development and a potential nanomaterial path forward. *Nature Nanotechnology* **2020,** *15* (8), 646-655.

29. Pilkington, E. H.; Suys, E. J. A.; Trevaskis, N. L.; Wheatley, A. K.; Zukancic, D.; Algarni, A.; Al-Wassiti, H.; Davis, T. P.; Pouton, C. W.; Kent, S. J.; Truong, N. P., From influenza to COVID-19: Lipid nanoparticle mRNA vaccines at the frontiers of infectious diseases. *Acta Biomaterialia* **2021,** *131*, 16-40.

30. Liu, S.; Cheng, Q.; Wei, T.; Yu, X.; Johnson, L. T.; Farbiak, L.; Siegwart, D. J., Membrane-destabilizing ionizable phospholipids for organ-selective mRNA delivery and CRISPR–Cas gene editing. *Nature Materials* **2021,** *20* (5), 701-710.

31. Gilleron, J.; Querbes, W.; Zeigerer, A.; Borodovsky, A.; Marsico, G.; Schubert, U.; Manygoats, K.; Seifert, S.; Andree, C.; Stöter, M.; Epstein-Barash, H.; Zhang, L.; Koteliansky, V.; Fitzgerald, K.; Fava, E.; Bickle, M.; Kalaidzidis, Y.; Akinc, A.; Maier, M.; Zerial, M., Image-based analysis of lipid nanoparticle–mediated siRNA delivery, intracellular trafficking and endosomal escape. *Nature Biotechnology* **2013,** *31* (7), 638-646.

32. Sahay, G.; Querbes, W.; Alabi, C.; Eltoukhy, A.; Sarkar, S.; Zurenko, C.; Karagiannis, E.; Love, K.; Chen, D.; Zoncu, R.; Buganim, Y.; Schroeder, A.; Langer, R.; Anderson, D. G., Efficiency of siRNA delivery by lipid nanoparticles is limited by endocytic recycling. *Nature Biotechnology* **2013,** *31* (7), 653-658.

33. Jahn, R.; Scheller, R. H., SNAREs — engines for membrane fusion. *Nature Reviews Molecular Cell Biology* **2006,** *7* (9), 631-643.

34. Chen, Y. A.; Scheller, R. H., SNARE-mediated membrane fusion. *Nature Reviews Molecular Cell Biology* **2001,** *2* (2), 98-106.

35. Akinc, A.; Maier, M. A.; Manoharan, M.; Fitzgerald, K.; Jayaraman, M.; Barros, S.; Ansell, S.; Du, X.; Hope, M. J.; Madden, T. D.; Mui, B. L.; Semple, S. C.; Tam, Y. K.; Ciufolini, M.; Witzigmann, D.; Kulkarni, J. A.; van der Meel, R.; Cullis, P. R., The Onpattro story and the clinical translation of nanomedicines containing nucleic acid-based drugs. *Nature Nanotechnology* **2019,** *14* (12), 1084-1087.

36. Kulkarni, J. A.; Witzigmann, D.; Leung, J.; van der Meel, R.; Zaifman, J.; Darjuan, M. M.; Grisch-Chan, H. M.; Thöny, B.; Tam, Y. Y. C.; Cullis, P. R., Fusion-dependent formation of lipid nanoparticles containing macromolecular payloads. *Nanoscale* **2019,** *11* (18), 9023-9031.

37. Eygeris, Y.; Patel, S.; Jozic, A.; Sahay, G., Deconvoluting Lipid Nanoparticle Structure for Messenger RNA Delivery. *Nano Letters* **2020,** *20* (6), 4543-4549.

38. Patel, S.; Ashwanikumar, N.; Robinson, E.; Xia, Y.; Mihai, C.; Griffith, J. P.; Hou, S.; Esposito, A. A.; Ketova, T.; Welsher, K.; Joyal, J. L.; Almarsson, Ö.; Sahay, G., Naturally-occurring cholesterol analogues in lipid nanoparticles induce polymorphic shape and enhance intracellular delivery of mRNA. *Nature Communications* **2020,** *11* (1), 983.

39. Hou, X.; Zaks, T.; Langer, R.; Dong, Y., Lipid nanoparticles for mRNA delivery. *Nature Reviews Materials* **2021,** *6* (12), 1078-1094.

40. Kanasty, R.; Dorkin, J. R.; Vegas, A.; Anderson, D., Delivery materials for siRNA therapeutics. *Nature Materials* **2013,** *12* (11), 967-977.

41. Huang, Y.; Wang, T.; López, M. E. U.; Hirano, M.; Hasan, A.; Shin, S. R., Recent advancements of human iPSC derived cardiomyocytes in drug screening and tissue regeneration. *Microphysiol. Syst.* **2020,** *4*.

42. Wagner, J. U. G.; Pham, M. D.; Nicin, L.; Hammer, M.; Bottermann, K.; Yuan, T.; Sharma, R.; John, D.; Muhly-Reinholz, M.; Tombor, L.; Hardt, M.; Madl, J.; Dimmeler, S.; Krishnan, J., Dissection of heterocellular cross-talk in vascularized cardiac tissue mimetics. *Journal of Molecular and Cellular Cardiology* **2020,** *138*, 269-282.

43. Hassett, K. J.; Benenato, K. E.; Jacquinet, E.; Lee, A.; Woods, A.; Yuzhakov, O.; Himansu, S.; Deterling, J.; Geilich, B. M.; Ketova, T.; Mihai, C.; Lynn, A.; McFadyen, I.; Moore, M. J.; Senn, J. J.; Stanton, M. G.; Almarsson, Ö.; Ciaramella, G.; Brito, L. A., Optimization of Lipid Nanoparticles for Intramuscular Administration of mRNA Vaccines. *Molecular Therapy - Nucleic Acids* **2019,** *15*, 1-11.

Supporting information

a

CPE4

CPK4

ALC0315

SM102

b
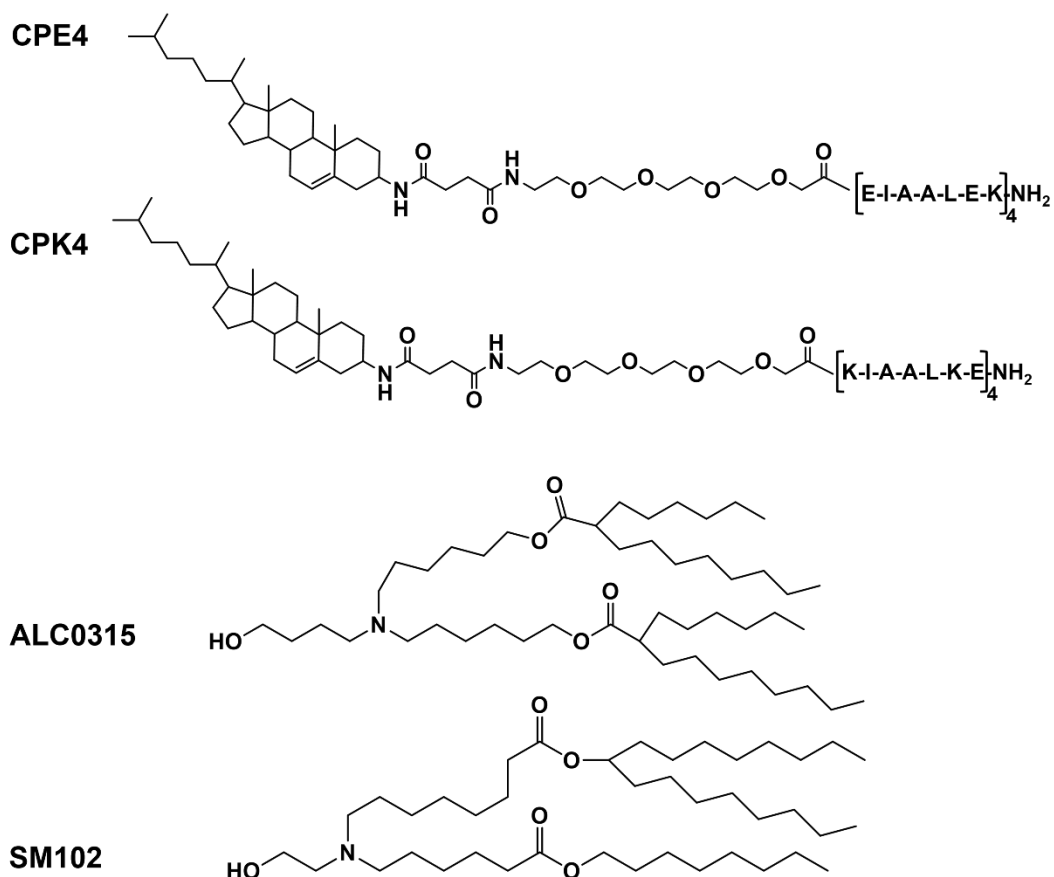
Lipid compositions of LNPs (mol%).				
	ALC0315-CPE4	ALC0315	SM102-CPE4	SM102
ALC0315	50	50	/	/
SM102	/	/	50	50
Cholesterol	37.5	38.5	37.5	38.5
DSPC	10	10	10	10
DMG-PEG2K	1.5	1.5	1.5	1.5
CPE4	1	/	1	/

c

Characterization of LNP formulations.				
LNPs	Hydrodynamic diameter (nm)	PDI	Zeta potential (mV)	EE (%)
ALC0315-CPE4	98.5±2.3	0.154±0.05	-7.29±0.88	81.15±5.35
ALC0315	86.6±3.8	0.132±0.024	-4.01±0.66	90.20±2.71
SM102-CPE4	116.2±1.4	0.134±0.05	-8.13±0.68	82.48±3.47
SM102	95.55±2.7	0.172±0.024	-5.36±0.61	89.54±2.35

SI Figure 1 (a) Structures of CPE4, CPK4, and lipids ACL0315 and SM107 used for the preparation of LNPs. **(b)** Lipids compositions of LNPs**. (c)** Characterization of LNPs.